MECHANICAL PERFORMANCE OF WROUGHT ALLOY 718 WITH DIFFERENT GRAIN SIZES IN HOT CORROSIVE ENVIRONMENT

M. Yoshiba

Department of Precision Engineering
Tokyo Metropolitan University
Minami-Ohsawa 1-1, Hachioji, Tokyo 192-03, Japan

Abstract

In order to assess an applicability of Alloy 718 in the corrosive environment at the elevated temperature more than customarily used, both the creep and the fatigue performances were investigated of it with different grain sizes at 1073K in the Na_2SO_4-NaCl molten salt environment, together with an establishment of the corrosion map for the V_2O_5-Na_2SO_4-NaCl molten salt system. Alloy 718 was found to have much better resistance against the Na_2SO_4-induced hot corrosion without an occurrence of an intergranular attack as compared with the other Ni-rich superalloys such as Alloy 751, although the former was subjected more heavily to the V_2O_5-induced vanadium pentoxide attack. Creep rupture strength degradation due to hot corrosion was most mitigated in almost all the superalloys, mainly by virtue of an effective suppression of aggressive intergranular penetration of the low melting Ni sulfide liquids. Furthermore, a grain coarsening was found to be effective for improving the creep rupture properties even in hot corrosive environment without increasing a corrosion sensitivity. A corrosion-induced fatigue strength degradation of Alloy 718 was more significant than the case of creep, but its degree was rather mitigated than Alloy 751. A corrosion sensitivity of the fatigue strength was also found to be nearly independent of a grain size.

Superalloys 718, 625 and Various Derivatives
Edited by Edward A. Loria
The Minerals, Metals & Materials Society, 1991

Introduction

Alloy 718 is certainly one of the most widely used of the Ni-base superalloys today. However, its application has been limited at cryogenic temperatures up to approximately 923K, mainly because of a rapidly decreased structural stability, in particular of a γ'' phase [Ni_3Nb], at the more elevated temperature (1). Then a microstructural control of the wrought Alloy 718 has been focused on developing a fine grain size in order to attain much increased strength properties such as tensile and fatigue strengths in the cryogenic temperature regime, by means of increasing a hardness which is associated with a development of γ'' phase.

On the other hand, Alloy 718 is known to have an appreciably better high temperature corrosion resistance in the aggressive environments, in particular against a hot corrosion, as compared with the other more Ni-rich superalloys (2, 3). Therefore, it seems to have a potential for the successful use both in the higher temperature regime and in such aggressive environments. In this case, an advantage of the rather coarse grain size should be expected particularly for the improved high temperature creep rupture properties.

In the present study, in order to assess an applicability of Alloy 718 as a structural alloy in the aggressive environments at the more elevated temperature, two kinds of the mechanical properties of creep and fatigue were investigated for it with different grain sizes in the laboratorically simulated hot corrosive environment.

Experimental

Materials

Two kinds of Ni-base superalloys were used in the present study; one is Alloy 718 and the other is Alloy 751 for comparison. These chemical compositions are listed in Table I. Two kinds of heat treatments were adopted for each alloy to develop different microstructures including a grain size, as shown in Table II. For Alloy 718, in particular, the SEM micrographs after two ways of heat treatments are shown in Fig. 1. Here, a fine-grained (FG) specimen, which was applied with a specification heat treatment for an improved cryogenic temperature strength, has a microstructure typical for this alloy, consisting of both very fine γ'' particles within a grain and coarse δ [Ni_3Nb] in the grain boundary region along with small amount of Mo- and Nb-rich MC carbide. On the other hand, a coarse-grained (CG) specimen has a microstructure consisting of rather large and cellular γ'' within a grain together with the grain boundary precipitates including δ and M_6C carbide (1).

On the contrary, Alloy 751 has an essentially similar microstructure between different kinds of heat treatments (solution treatments) adopted except for a difference in a grain size; both ways of heat treatments result in a typical microstructure consisting of great numbers of fine γ' [$Ni_3(Ti,Al)$] in a grain and the Cr-rich $M_{23}C_6$ grain boundary carbides.

Table I Chemical Compositions of Superalloys Used (Mass %).

Alloys	C	Si	Mn	S	Ni	Cr	Ti	Al	Mo	Nb+Ta	Fe
Alloy 718	0.03	0.11	0.22	0.005	Bal.	17.54	0.92	0.42	3.02	4.99	18.54
Alloy 751	0.09	0.20	0.53	0.007	Bal.	16.07	2.05	1.10	-	1.18	5.74

Table II Heat Treatment Conditions and the Corresponding Grain Size and Vickers Hardness Number.

Alloy-Symbols	Heat Treatment Conditions	Grain Size (μm)	HV(196N)
Alloy 718-FG	1273K×1h→AC + 993K×8h→FC(873K)→AC.	15	441
Alloy 718-CG	1373K×2h→WQ + 1073K×24h→AC.	145	341
Alloy 751-FG	1373K×2h→WQ + 1073K×24h→AC.	44	313
Alloy 751-CG	1473K×2h→WQ + 1073K×24h→AC.	125	306

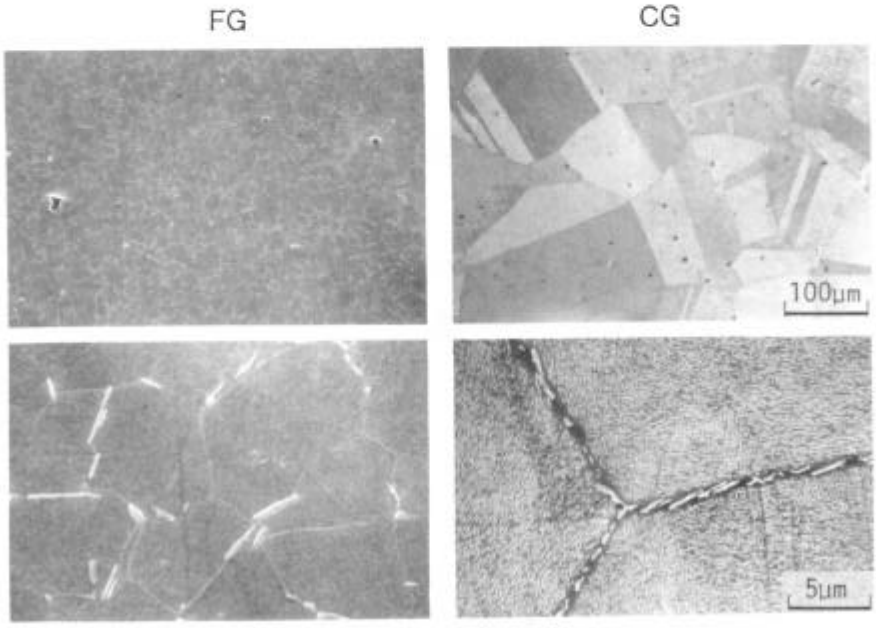

Figure 1 - Typical microstructures of Alloy 718 after two ways of heat treatments.

Experimental Procedures

High temperature corrosion tests were conducted by means of the salt coating method, using the sylindrical specimens with dimensions of 15 mm in diameter and 10 mm in length. In order to simulate a variety of the actual molten salt corrosive environments such as hot corrosion and so-called vanadium pentoxide attack in the laboratory, various compositions of the V_2O_5-Na_2SO_4-NaCl salt mixtures were coated onto the specimen surface. The amount of salt mixture coated was 0.2 kg/m². The corrosion tests were carried out at 1123K for 20h, at which almost all the synthetic salt mixtures can be melted except for a pure Na_2SO_4 (m.p.=1157K). After the corrosion tests, specimens were descaled by an electrochemical technique in the molten Na_2CO_3-NaOH salt, and a corrosion mass loss was determined as a measure of the corrosion resistance.

Creep rupture tests were performed at 1073K which is considered for Alloy 718 a critical temperature available for a structural alloy. The specimens with dimensions of 5 mm in dia. and 30 mm in gage length were coated with the 90%Na_2SO_4-10%NaCl salt mixture, corresponding to a very severe hot corrosive environment at the testing temperature (4). The amount precoated was 0.4 kg/m² and the repeated salt coating was made at every 200h to maintain a corrosive action for a long period. The tests in static air were also done using the specimens without a salt coating.

High cycle fatigue tests also were carried out at 1073K, using the smooth bar specimens with 8 mm in dia. and 15 mm in gage length, by means of the rotating-bending fatigue testing machines (1500 rpm). The composition and amount of the salt mixture coated on the specimen are similar to the case of the creep rupture test, except for a difference in the frequency of repeated coating; at every 3 x 10^5 cycles for the fatigue test.

After the different tests, metallographic examinations were made on the sections of surface scale and alloy substrate by means of an optical microscopy and an electron probe X-ray microanalysis (EPMA). The observation of the fracture surface also was conducted by a scanning electron microscopy (SEM).

Results and Discussion

High Temperature Corrosion Resistance

Figure 2 shows the isocorrosion contours; the corrosion map, for Alloy 718 (FG) together with Alloy 751 (CG), obtained from the coating tests at 1123K for 20h using the V_2O_5-Na_2SO_4-NaCl systems of salt mixtures. It can be seen that Alloy 718 shows a characteristic corrosion performance in contrast to the case of Alloy 751. Alloy 718 has a markedly increased resistance against a Na_2SO_4-induced hot corrosion as compared with that of Alloy 751. In such the Na_2SO_4-rich salt environments, both Nb and Mo in Alloy 718 can be considered harmless, even though they are generally regarded as rather detrimental elements to hot corrosion (6, 7).

However, Alloy 718 was also found to undergo more heavily a vanadium pentoxide attack in the V_2O_5-rich salt environments rather than Alloy 751. The reasoning for such a result is exactly unclarified, but the same result has been obtained for the same system of Fe-42Ni-15Cr alloys newly developed by the author (7). Fitzer and Schwab (8) have shown that Fe-Ni alloys containing Ni up to 40% have rather lowered resistance against the V_2O_5-induced attack than pure Ni, and in particular an Invar alloy consisting of Fe-36%Ni exhibits an exceptionally minimized corrosion resistance. Then an increased susceptivility of Alloy 718 to vanadium pentoxide attack should be considered intrinsic for its basic composition of Ni- and Fe-rich. Anyhow, Alloy 718 is characterized by a much improved corrosion performance in the Na_2SO_4-rich hot corrosive environment, although its applicability is markedly reduced in both the V_2O_5-rich and the NaCl-rich environments.

Figure 3 shows the typical corrosion morphologies at the cross-sections of Alloy 718 specimens corrosion-tested at 1123K for 20h in two kinds of the representative molten salt environments. It was confirmed for Alloy 718 to exhibit in general an uniform corrosion morphology in almost all the corrosive environments. Hot corrosive environment is generally known as highly capable of inducing a preferential intergranular attack for many kinds of Ni-base superalloys including Alloy 751, but for Alloy 718 it can induce only a general corrosion, although an internal corrosion (sulphidation) is inevitably occurred in such an environment (2, 3). This suggests for Alloy 718 to have an essentially stable grain boundary with a minimized susceptibility to an intergranular attack.

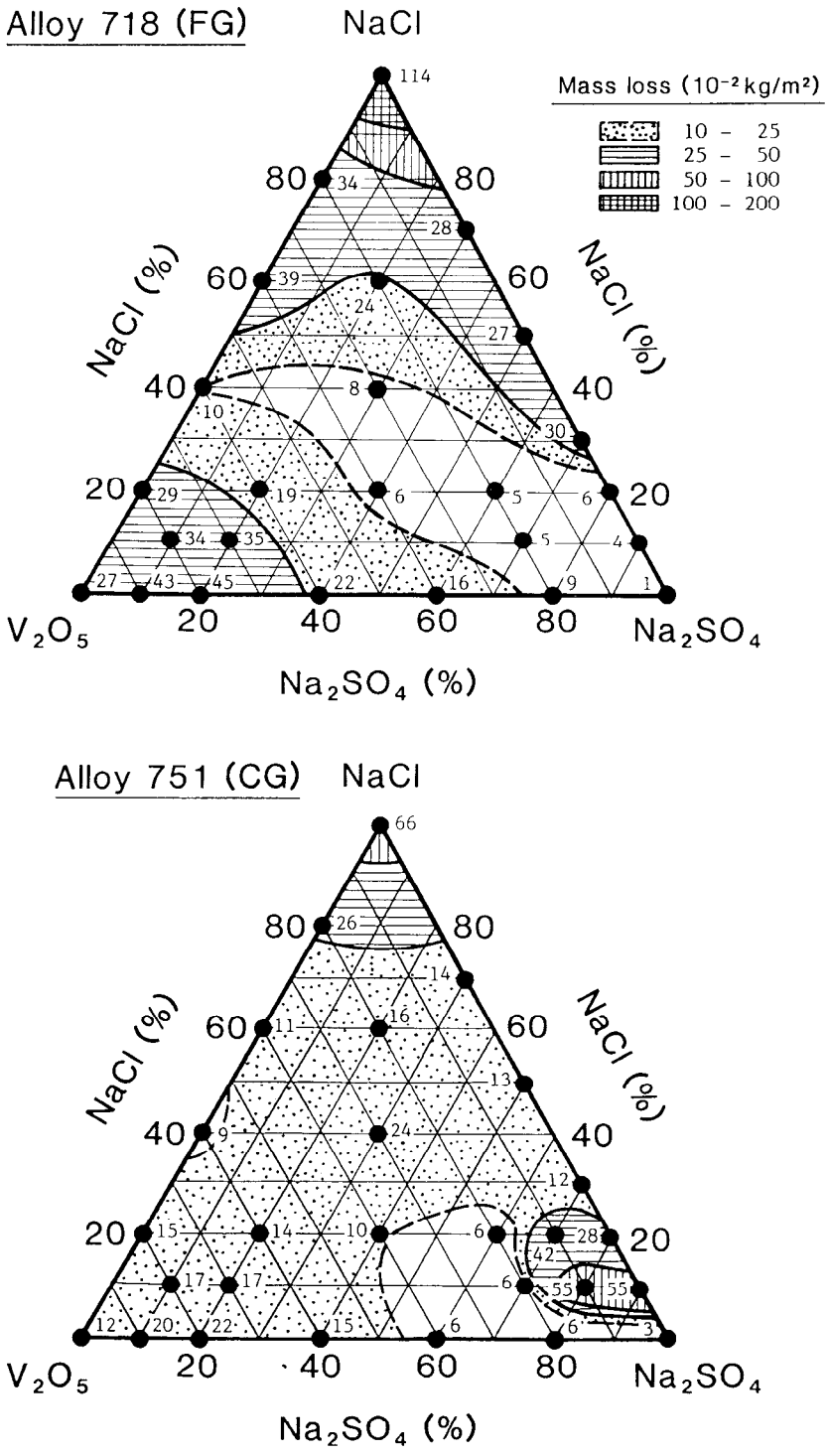

Figure 2 - Isocorrosion contours of Alloy 718 (FG) and Alloy 751 (CG) in the salt coating test at 1123K for 20h using various compositions of the V_2O_5-Na_2SO_4-NaCl salt mixtures.

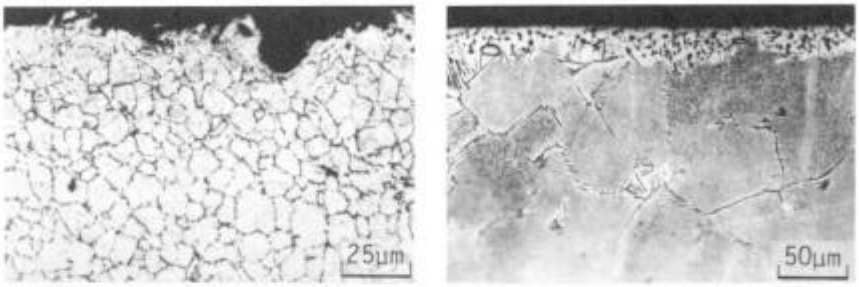

Figure 3 - Typical corrosion morphologies at the cross-sections of Alloy 718 specimens after the corrosion tests at 1123K for 20h followed by a descaling.

Creep Rupture Properties in Hot Corrosive Environment

Figure 4 shows typical creep curves of Alloy 718 specimens with different grain sizes at 1073K in air and in hot corrosive environment. It is apparent that hot corrosive environment alters only little a creep rupture behavior of both FG and CG specimens, since the creep curves are essentially similar between in air and in hot corrosive environment. As regards a comparison between FG and CG specimens, the former is ruptured in the more ductile manner, although a disadvantage of the former in the rupture life is pronounced, as compared with the latter.

Figure 5 shows the stress rupture properties of Alloy 718 specimens with different grain sizes at 1073K in air and in hot corrosive environment. It should be noted again that Alloy 718 shows the least corrosion-induced rupture life shortening regardless of a grain size. The CG specimens exhibited a generally improved creep rupture strength level rather than the FG specimens, and such a difference in the rupture strength becomes more pronounced in the lower stress and longer life regime. On the other hand, a reduction of the rupture elongation due to hot corrosion is rather pronounced in FG specimens, but the rupture ductility itself was maintained still enough even in the aggressive environment.

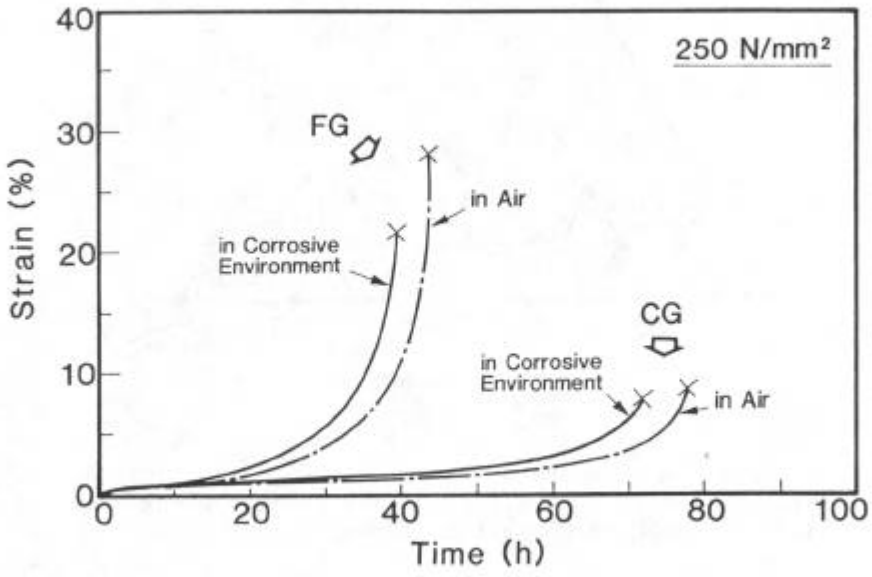

Figure 4 - Typical creep curves of Alloy 718 with different grain sizes at 1073K in air and in hot corrosive environment.

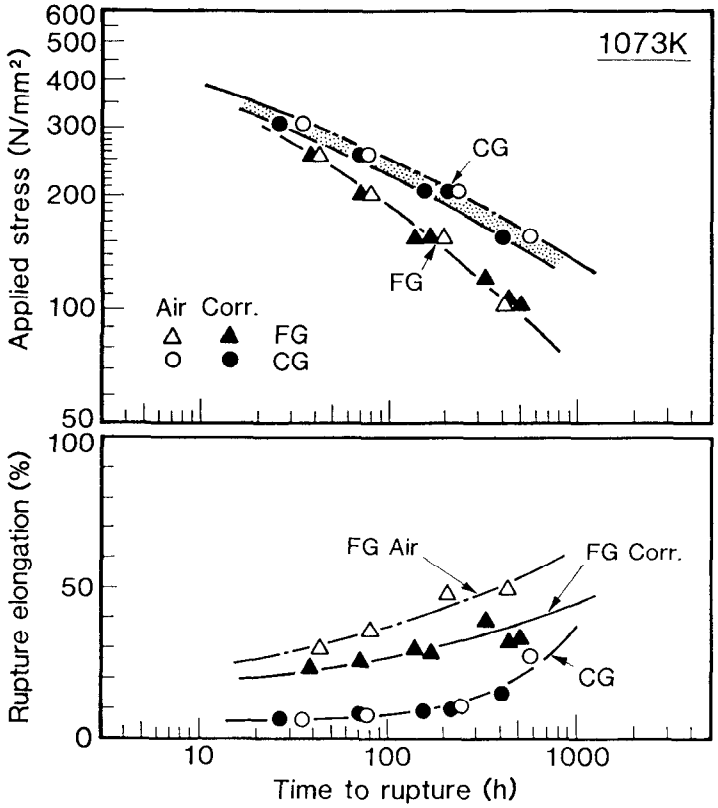

Figure 5 Creep rupture properties of Alloy 718 with different grain sizes at 1073K in air and in hot corrosive environment.

By the way, the rupture ductility was found to increase unexpectedly as the creep rupture life is extended. This should be attributed to an overaging due to the prolonged heating at 1073K. Thus such a high temperature heating tends to promote an alloy softening by virtue of the microstructural modification.

The 100h creep rupture strength data for Alloy 718 were summarized in Table Ⅲ, together with those for Alloy 751 for comparison. It is evident that the corrosion-induced creep rupture strength degradation can be more effectively restrained in Alloy 718 rather than in Alloy 751, since the former exhibits much higher corrosion rupture strength ratio of 0.92. It has been already revealed by the authors previous study that Alloy 718 has the minimized corrosion sensitivity of the creep rupture strength among many kinds of the commercial heat resisting Fe-Ni-Cr alloy system (9). Furthermore, for Alloy 718 the grain coarsening results in the increased rupture strength both in air and in hot corrosive environment without a detrimental effect on the corrosion sensitivity. This is in contrast with the case for Alloy 751 in which the grain coarsening brings about a markedly lowered corrosion rupture strength ratio of 0.27. Such an advantage of the grain coarsening for an improved creep rupture strength should be reasonably explained by considering an increasing difficulty for a diffusion-controlled recovery process. Anyhow, increasing a grain size is much effective for Alloy 718 to improve the creep rupture strength not only in air but also in hot corrosive environment.

Figure 6 shows typical creep rupture morphologies of Alloy 718 with different grain sizes in hot corrosive environment. Creep rupture of this alloy was found to be caused in the essentially same manner as in

Table III Summary of the Creep Rupture Strength Properties for Alloy 718 and Alloy 751 with Different Grain Sizes at 1073K in Air and in Hot Corrosive Environment.

Alloy-Symbols	100h-Rupture Strength (N/mm^2)		100h-Corrosion Rupture Strength Ratio (B/A)
	Air (A)	Corr. Env. (B)	
Alloy 718-FG	185	170	0.92
Alloy 718-CG	240	220	0.92
Alloy 751-FG	245	100	0.41
Alloy 751-CG	260	70	0.27

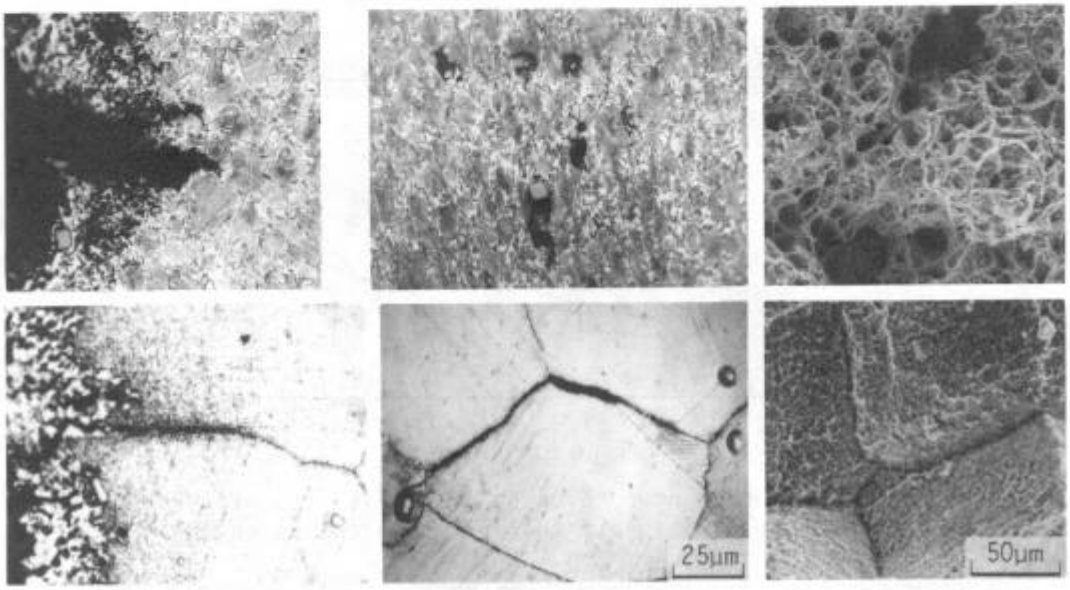

Figure 6 - Creep rupture morphologies of Alloy 718 with different grain sizes at 1073K in hot corrosive environment. Stress axis is vertical. (FG: 150 N/mm^2, t_r=163h, CG: 250 N/mm^2, t_r= 74h)

air; through the growth and coalescence of both the internal grain boundary cracks induced by a mechanical creep damage (grain boundary sliding) and the surface grain boundary cracks affected to some degree by the corrosive environment, independently of a grain size. For Alloy 718, in particular, an intergranular attack was suppressed so much effectively that its enhancing effect on a surface crack propagation was minimized (9).

This is in contrast with the case for Alloy 751 in which an intergranular penetration of the low melting Ni sulfides such as Ni-Ni_3S_2 eutectic is capable of being induced so rapidly and preferentially under the applied stress as to produce a much weaker grain boundary to be later a main crack and to cause directly a premature fracture in a brittle manner, prior to an initiation of the creep-induced internal grain boundary crack (9, 10). Then, the significantly corrosion-induced strength degradation in Alloy 751, as already shown in Table III, is closely related to such an increased significance of intergranular attack in the creep rupture process.

Figure 7 shows the secondary electron and characteristic X-ray images at the tip of an intergranular attack in Alloy 718-CG specimen creep-ruptured at 1073K in hot corrosive environment. As can be seen, an intergranular attack accompanied by an oxychlorination-dominating reaction process proceeds predominantly, and no sulfide plays important role in

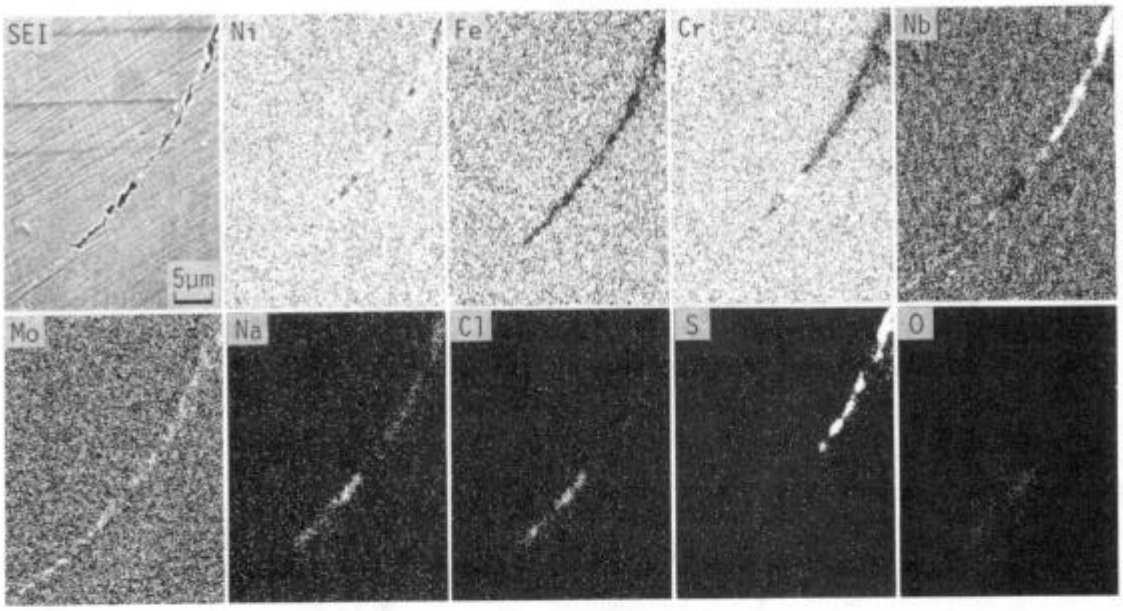

Figure 7 - Secondary electron and characteristic X-ray images at the tip of an intergranular attack in Alloy 718 (CG) specimen creep-ruptured under 250 N/mm² for 74h at 1073K in hot corrosive environment. Stress axis is horizontal.

this alloy. It is surprising that an intergranular penetration can occur almost freely from the sulfide, at least at a front of the attack, since many kinds of Ni-base superalloys including Alloy 751 have been found to undergo a sulfide-preceding severe intergranular attack in this temperature region (9-11). Consequently, an effectively suppressed intergranular attack in Alloy 718 should be associated with a markedly reduced responsibility of sulfides.

Figure 8 shows the characteristic X-ray profiles across the grain boundary carbides in the Alloy 718-FG and -CG specimens. It was revealed by EPMA that the grain boundary carbide precipitates are mainly composed of Mo and Nb in spite of differences in the heat treatment and thermal hysteresis between FG and CG specimens. It should be noted that the grain boundary carbide precipitates are Cr-free for Alloy 718. The Cr-rich boundary carbide precipitation has been found to result in a development of the Cr-depleted zone adjacent to the grain boundary, which is capable of inducing a formation of the low melting Ni sulfides such as Ni-Ni_3S_2 eutectic (12). The result for Alloy 751 is a just real effect. However, Alloy 718 has inherently lowered potential for the low melting Ni sulfide formation.

Whitlow et al. (13) have suggested that both a microalloying and a microstructural control in the grain boundary region are very important factor to determine the creep rupture properties of Ni-base superalloys in a molten salt corrosive environment. For Alloy 718, anyhow, an aggressive intergranular attack associated with a Ni sulfide formation can be effectively suppressed, so that a corrosion-induced creep rupture strength degradation should be minimized.

Fatigue Strength Properties in Hot Corrosive Environment

Figure 9 shows the S-N curves (Wöhler curves) obtained from the fatigue tests at 1073K both in air and in hot corrosive environment for Alloy 718 with different grain sizes. It can be seen that hot corrosive environment

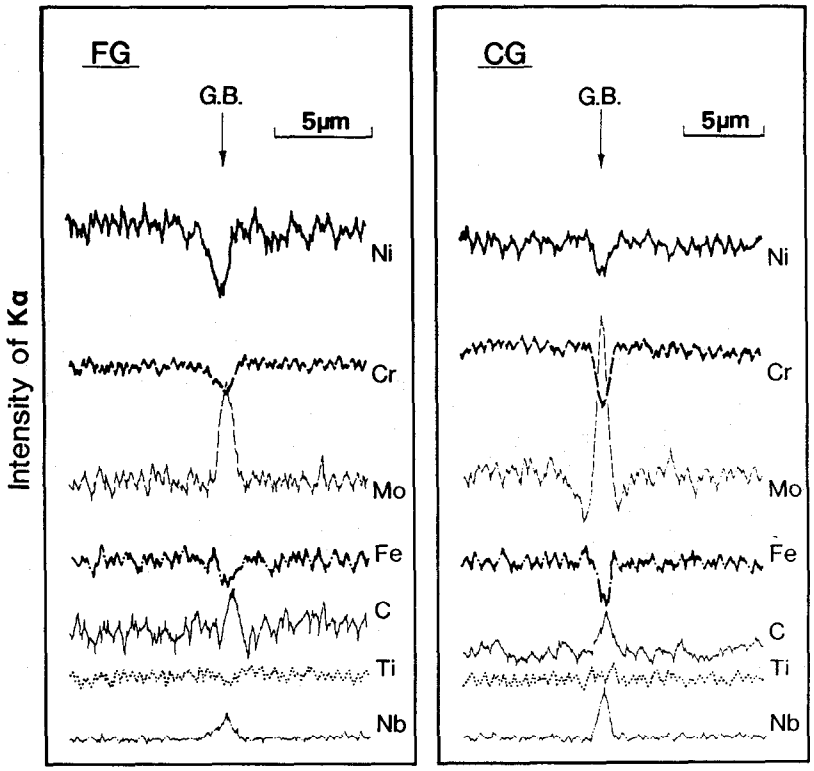

Figure 8 - Characteristic X-ray profiles across the grain boundary (carbides) in Alloy 718 specimens with different grain sizes.
(FG: as heat-treated, CG: creep-ruptured under 250 N/mm² for 74h)

is so aggressive as to induce a marked reduction of the fatigue life, regardless of a grain size. However, such a corrosion-induced fatigue life degradation is rather mitigated as a stress (amplitude) level is much lowered. This is in contrast with the case for Alloy 751 in which a corrosion-induced fatigue life shortening became more significant in the lower stress region (14). Furthermore, the fatigue properties for Alloy 718 are also characterized by having an almost equivalent strength level regardless of a grain size both in air and in hot corrosive environment.

The data of fatigue strength properties for Alloy 718 were summarized in Table IV, together with those for Alloy 751 for comparison. It is clear again that Alloy 718 is in a nearly equivalent fatigue strength level between two kinds of grain sizes both in air and in hot corrosive environment, so that the corrosion fatigue strength ratio (B/A in Table IV) is hardly dependent on a grain size. On the contrary, the corrosion fatigue properties for Alloy 751 depend strongly upon a grain size; decreasing a grain size results in an enhanced corrosion sensitivity of the fatigue strength so as for a corrosion-induced strength degradation to be more significant, although the fatigue strength level in air is rather higher in the FG specimen.

In order to understand fully the fatigue strength properties, it is important to clarify the fatigue fracture behavior such as an initiation and a propagation of the fatigue crack, since it should be the most important factor determining the fatigue life. Figure 10 shows the initiation and propagation behavior of the fatigue cracks for Alloy 718 in air and in hot corrosive environment, which was obtained from the microstructural measurement of the interrupted fatigue specimens. It is evident that hot corrosive environment brings about a premature fatigue crack initiation

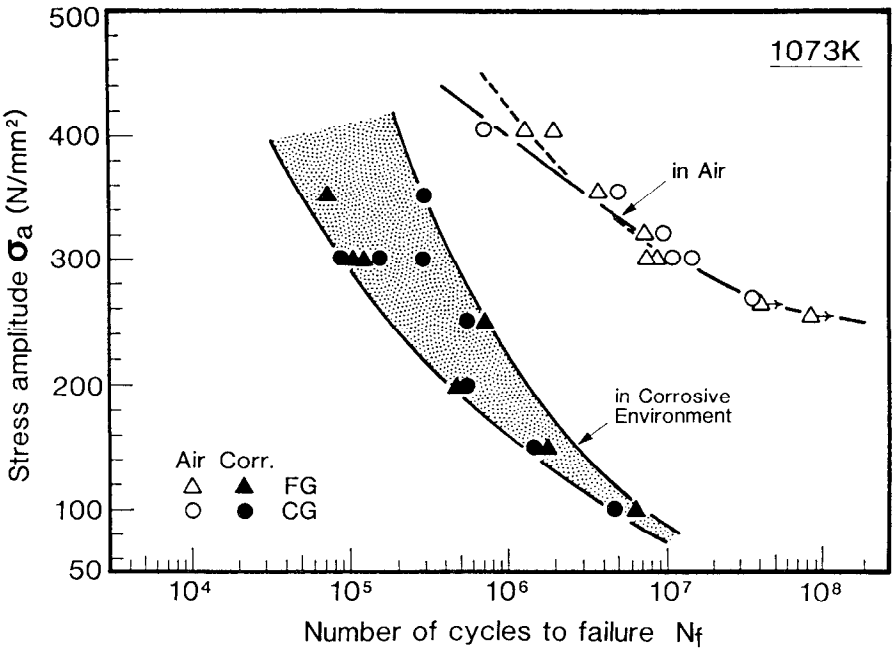

Figure 9 - S-N curves of Alloy 718 with different grain sizes at 1073K in air and in hot corrosive environment.

Table IV Summary of the Fatigue Strength Properties for Alloy 718 and Alloy 751 with Different Grain Sizes at 1073K in Air and in Hot Corrosive Environment.

Alloy-Symbols	10^6Cycle Fatigue Strength (N/mm²)			10^7Cycle Fatigue Strength (N/mm²)		
	Air (A)	Corr. (B)	(B/A)	Air (A)	Corr. (B)	(B/A)
Alloy 718-FG	440	175	0.40	295	85	0.29
Alloy 718-CG	390	165	0.42	305	75	0.25
Alloy 751-FG	390	150	0.38	320	20	0.06
Alloy 751-CG	365	210	0.58	330	50	0.15

at the grain boundary in almost all the case, regardless of a grain size. This can be reasonably explained by considering an intergranular attack-induced crack initiation (14). Furthermore, it is characteristic for Alloy 718 that the initiation and propagation behavior including their paths of the corrosion fatigue cracks are essentially similar between the FG and CG specimens; in both specimens the predominant fatigue cracks tend to propagate along the grain boundaries. However such a propagation rate of the intergranular cracks is not so rapid as to cause promptly a catastrophic failure as soon as it initiates. This is in contrast with the case for the fine-grained Alloy 751 specimens, in which a rapid propagation of the intergranular crack is permitted because of the combined effect of the mechanical fatigue and chemical corrosive damages focused on the grain boundary (14).

It was revealed by EPMA that for Alloy 718 an intergranular attack preceding a fatigue crack is oxychloride-dominating regardless of a grain size. This is essentially similar to the case of creep, as already shown in Fig. 7, and is in contrast with a result of the work by Floreen and Kane (15). They have suggested on the basis of the experimental work about a fatigue crack propagation behavior in the fine-grained Alloy 718 at 923K using different compositions of gaseous environments that the sulfur containing environments tend to enhance markedly the propagation rate of

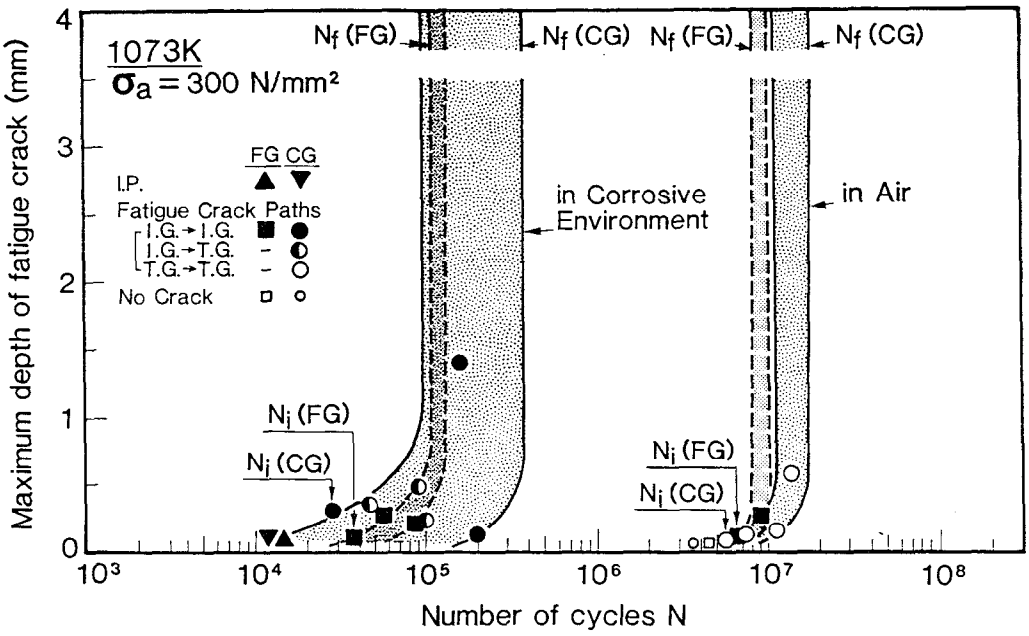

I.P. : Intergranular Penetration, I.G. : Intergranular, T.G. : Transgranular

Figure 10 - Initiation and propagation behavior of Alloy 718 with different grain sizes at 1073K in air and in hot corrosive environment.

intergranular crack probably due to the formation of the low melting Ni-Ni_3S_2 eutectic liquids. In the present study, however, a sulfide has been revealed to play no important role in the fatigue crack propagation process. Then the relatively mitigated fatigue strength degradation for Alloy 718 due to hot corrosion seems to be related to such a sulfide-free fatigue crack propagation behavior. Furthermore, a grain size independence of the corrosion fatigue strength should be attributed to the facts that a fracture mode was essentially same; intergranular, regardless of a grain size, and that an intergranular attack susceptibility was effectively minimized for Alloy 718.

Concluding Remarks

1) Alloy 718 was found to have a much better resistance against the Na_2SO_4-induced hot corrosion as compared with the more Ni-rich Alloy 751, although the former undergoes more heavily a vanadium pentoxide attack than the latter. It was also confirmed for Alloy 718 to exhibit in general an uniform corrosion morphology without an intergranular attack almost all the corrosive salt environments.

2) The creep rupture strength degradation due to hot corrosion was minimized for Alloy 718 mainly by virtue of an effective suppression of an intergranular penetration of sulfides. A corrosion sensitivity of the creep rupture strength was independent to a grain size in contrast to the case for Alloy 751. Then the grain coarsening should be much effective for the improved creep rupture strength properties not only in air but also in hot corrosive environment.

3) Hot corrosion was found to bring about a more significant fatigue strength degradation for Alloy 718 rather than the case of creep. However, the degree of strength degradation was mitigated rather than the case for Alloy 751. Both a corrosion sensitivity of the fatigue strength and the

corrosion fatigue strength itself were also found to hardly depend on a grain size.

Acknowledgments

The author wish to acknowledge Mr. T. Masaki of Shimadzu Corp. for the valuable analyses by EPMA. The experimental work in the present study was competently carried out by M. Eng. H. Mizuno, Messrs. M. Ushiki, T. Ishii, J. Izumi and H. Tanabe, who were formerly undergraduates at Tokyo Metropolitan University.

References

1. E. E. Brown and D. R. Muzyka, "Nickel-Iron Alloys", in Superalloys II, ed. by C. T. Sims, N. S. Stoloff and W. C. Hagel, (NY, J. Wiley & Sons, 1987), 165-188.

2. R. Viswanathan, "High Temperature Corrosion of Some Gas Turbine Alloys", Corrosion, 24(1968), 359-368.

3. M. Yoshiba, O. Miyagawa and H. Fujishiro, "Hot Corrosion Behavior of Heat Resisting Alloys", J. Iron Steel Inst. Japan (in Japanese), 67 (1981), 996-1005.

4. D. W. McKee, D. A. Shores and K. L. Luthra, "The Effect of SO_2 and NaCl on High Temperature Hot Corrosion", J. Electrochem. Soc., 125(1978), 411-419.

5. J. Stringer and D. P. Whittle, "The Hot Corrosion of Nickel-Base Superalloys -The Effect of Molten Salt Chemistry", in Metal-Slag-Gas Reactions and Processes, ed. by Z. A. Foroulis and W. W. Smeltzer, (Princeton, Electrochem. Soc., 1975), 665-677.

6. F. S. Pettit and C. S. Giggins, "Hot Corrosion", in Superalloys II, ed. by C. T. Sims, N. S. Stoloff and W. C. Hagel, (NY, J. Wiley & Sons., 1987), 327-358.

7. M. Yoshiba, O. Miyagawa and H. Fujishiro, "High Temeperature Performance of New Nickel-Iron-Base Superalloys in Aggressive Environments", in Proc. MRS International Meeting on Advanced Materials, ed. by M. Doyama, S. Somiya and R. P. H. Chang, Vol. 4 (Pittsburgh, MRS, 1989), 437-442.

8. E. Fitzer and J. Schwab, "Attack of Scaling-Resistant Materials by Vanadium Pentoxide and Effect of Various Alloying Elements Thereon", Corrosion, 12(1956), 459-464.

9. M. Yoshiba and O. Miyagawa, "Effect of Hot Corrosive Environment on Creep Rupture Properties of Commercial Iron-Nickel-Chromium Heat Resisting Alloys", in Proc. International Conference on Creep, (Tokyo, JSME, IMechE, ASME, ASTM, 1986), 193-198.

10. M. Yoshiba, "The Role of Applied Creep Stress on Hot Corrosion Behavior of a Nickel-Base Superalloy", in Proc. International Symposium on Solid State Chemistry of Advanced Materials, Part B: Workshop on High Temperature Corrosion of Advanced Materials and Protective Coatings, ed. by Y. Saito et al., (London, Elsevier, 1991), in press.

11. M. Yoshiba, O. Miyagawa, H. Mizuno and H. Fujishiro, "Effect of Environmental Factors on the Creep Rupture Properties of a Nickel-Base Superalloy Subjected to Hot Corrosion", Trans. Japan Inst. Metals, 29 (1988), 26-41.

12. O. Miyagawa and M. Yoshiba, "Effect of Zigzag Grain Boundaries on Creep Rupture Properties of a Nickel-Base Superalloy in Hot Corrosive Environment Induced by Na_2SO_4-NaCl Molten Salt", in Proc. 8th International Congress on Metallic Corrosion, Vol. 1 (Frankfurt, DECHEMA, 1981), 662-667.

13. G. A. Whitlow, G. C. Beck, R. Viswanathan and E. A. Crombie, "The Effects of a Liquid Sulfate/Chloride Environment on Superalloy Stress Rupture Properties at 704 ℃", Metall. Trans., 15A(1984), 23-28.

14. M Yoshiba and O. Miyagawa, "High Temperature Corrosion Fatigue and Grain Size Control in Nickel-Base and Nickel-Iron-Base Superalloys", in Superalloys 1988, ed. by S. Reichman et al., (Warrendale, The Metall. Soc., 1988), 825-834.

15. S. Floreen and R. H. Kane, "Effects of Environment on High-Temperature Fatigue Crack Growth in a Superalloy", Metall. Trans., 10A(1979), 1745-1751.